

1 **Title:**

2 Intra- and Inter-Specific Investigations of Skeletal DNA Methylation Patterns and Femur  
3 Morphology in Nonhuman Primates

4  
5 **Authors and Affiliations:**

6 Genevieve Housman<sup>1,2\*</sup>, Ellen E. Quillen<sup>3</sup>, and Anne C. Stone<sup>1,2</sup>

7  
8 <sup>1</sup>School of Human Evolution and Social Change, Arizona State University, Tempe, AZ, USA.

9 <sup>2</sup>Center for Evolution and Medicine, Arizona State University, Tempe, AZ, USA.

10 <sup>3</sup>Department of Genetics, Texas Biomedical Research Institute, San Antonio, TX, USA.

11

12 \*Corresponding author:

13 Genevieve Housman, Section of Genetic Medicine, University of Chicago, 920 East 58th Street,  
14 CLSC 317, Chicago, IL 60637, USA. Email: [ghousman@uchicago.edu](mailto:ghousman@uchicago.edu)

15

16 **Author Notes:**

17 Genevieve Housman is currently affiliated with the University of Chicago, and Ellen E. Quillen  
18 is currently affiliated with Wake Forest School of Medicine.

19

20 **Key Words:** DNA methylation, nonhuman primates, evolution, epigenome, bone

21 **Abstract:**

22 Epigenetic mechanisms influence the development and maintenance of complex  
23 phenotypes and may also contribute to the evolution of species-specific phenotypes. With respect  
24 to skeletal traits, little is known about the gene regulation underlying these hard tissues or how  
25 tissue-specific patterns are associated with bone morphology or vary among species. To begin  
26 exploring these topics, this study evaluates one epigenetic mechanism, DNA methylation, in  
27 skeletal tissues from five nonhuman primate species which display anatomical and locomotor  
28 differences representative of their phylogenetic groups. First, we test whether intra-specific  
29 variation in skeletal DNA methylation is associated with intra-specific variation in femur  
30 morphology. Second, we identify inter-specific differences in DNA methylation and assess  
31 whether these lineage-specific patterns may have contributed to species-specific morphologies.  
32 Specifically, we use the Illumina Infinium MethylationEPIC BeadChip to identify DNA  
33 methylation patterns in femur trabecular bone from baboons (n=28), macaques (n=10), vervets  
34 (n=10), chimpanzees (n=4), and marmosets (n=6). Significant differentially methylated positions  
35 (DMPs) were associated with a subset of morphological variants, but these likely have small  
36 biological effects and may be confounded by other variables associated with morphological  
37 variation. Conversely, several species-specific DMPs were identified, and these are found in  
38 genes enriched for functions associated with complex skeletal traits. Overall, these findings  
39 reveal that while intra-specific epigenetic variation is not readily associated with skeletal  
40 morphology differences, some inter-specific epigenetic differences in skeletal tissues exist and  
41 may contribute to evolutionarily distinct phenotypes.

42

43 **Introduction:**

44 Primates distinguish themselves from other mammals with their unique suite of  
45 anatomical features that initially enabled arboreal niche occupation and subsequently evolved to  
46 fit a myriad of habitats and forms of locomotion, the most unique being hominin bipedalism. The  
47 resulting morphological variation that has evolved across taxa has its foundation in underlying  
48 skeletal anatomies. Such skeletal morphologies are used to both characterize extant primate  
49 diversity and reconstruct the anatomy and locomotor capabilities of extinct primate species  
50 (Schultz 1930; Schultz 1937; Leigh and Shea 1995; Fleagle 1999; Ankel-Simons 2007). The  
51 range of mechanisms that enable the development of skeletal features are not entirely  
52 understood, though. Skeletal features related to varied body forms are often described as the  
53 result of environmental adaptations. However, skeletal morphology is more accurately defined as  
54 the result of complex processes, including environmental, genetic, and epigenetic mechanisms.  
55 While environmental (Henriksen et al. 2014; Lewton 2017; Lewton et al. 2018; Macrini et al.  
56 2013) and genetic (Smith et al. 2014; Joganic et al. 2017; Ritzman et al. 2017) factors have been  
57 readily explored, the important roles of epigenetic factors, such as DNA methylation, in skeletal  
58 tissue development and maintenance have only recently been identified (Delgado-Calle et al.  
59 2013; Goldring and Marcu 2012; García-Ibarbia et al. 2013; Liu et al. 2013; Loughlin and  
60 Reynard 2015; Ostanek et al. 2018; Ramos et al. 2014; Reynard et al. 2014; Reynard 2017;  
61 Simon and Jeffries 2017).

62 For instance, epigenetic processes are influential in regulating skeletal muscle  
63 development (Brand-Saber 2005; Palacios and Puri 2006; Pandorf et al. 2009; Zwetsloot et al.  
64 2009; Ling et al. 2012) which can impact the adjacent skeletal scaffolding system. Several genes  
65 involved in human skeletal development appear to be differentially methylated across fetal and  
66 adult developmental stages (de Andrés et al. 2013). Lastly, methylation variation in humans and

67 model organisms has been implicated in several skeletal pathologies and disorders, such as  
68 rheumatoid arthritis, osteoporosis, and osteoarthritis (Iliopoulos et al. 2008; Rivadeneira et al.  
69 2009; Bovée et al. 2010; Ralston and Uitterlinden 2010; Dimitriou et al. 2011; Goldring and  
70 Marcu 2012; Delgado-Calle et al. 2013; García-Ibarbia et al. 2013; Kasai et al. 2013; Liu et al.  
71 2013; Fernández-Tajes et al. 2014; den Hollander et al. 2014; Jeffries et al. 2014; Moazedi-  
72 Fuerst et al. 2014; Ramos et al. 2014; Reynard et al. 2014; Rushton et al. 2014; Loughlin and  
73 Reynard 2015; Jeffries et al. 2016; Morris et al. 2017; Reynard 2017). Some of these studies are  
74 the first to assess methylation patterns in human skeletal tissues (Delgado-Calle et al. 2013;  
75 García-Ibarbia et al. 2013; Fernández-Tajes et al. 2014; den Hollander et al. 2014; Jeffries et al.  
76 2014; Moazedi-Fuerst et al. 2014; Rushton et al. 2014), and such steps are important for truly  
77 identifying the relationship between epigenetic variation and skeletal phenotypic variation.

78 The contributions of epigenetics to primate phenotypic variation were first considered by  
79 King and Wilson (1975), who proposed that anatomical and behavioral differences between  
80 humans and chimpanzees were more likely “based on changes in the mechanisms controlling the  
81 expression of genes than on sequence changes in proteins” (King and Wilson 1975). Studies to  
82 understand methylation variation across species began soon afterwards (Gama-Sosa et al. 1983).  
83 General changes to mammalian epigenomes have been examined (Sharif et al. 2010), but most  
84 epigenetics work in primates has focused on humans – how it varies across distinct tissues within  
85 individuals (Lister et al. 2009; Sliker et al. 2013), across different individuals (Weksberg et al.  
86 2002; Petronis et al. 2003; Oates et al. 2006), across populations (Rakyan et al. 2004; Heyn et al.  
87 2013), in relation to aging processes (Fraga et al. 2005), and in relation to diet (Jacob et al. 1998;  
88 Rampersaud et al. 2000; Shelnut et al. 2004), as well as how it is inherited across generations  
89 (Suter et al. 2004; Flanagan et al. 2006; Gibbs et al. 2010; van Dongen et al. 2014). These studies  
90 have identified important within species methylation variants.

91 Similarly, epigenetic variation has been identified among primate species. Inter-specific  
92 variation in epigenetic signatures was initially inferred from underlying genomic sequences  
93 (Haygood et al. 2007; Prendergast et al. 2007; Bell et al. 2012). For instance, several promoter  
94 CpG densities vary across primates. These likely relate to regulatory methylation differences  
95 across species as primate CpG densities correlate with methylation levels (Weber et al. 2007).  
96 Additionally, gene expression studies, which primarily focus on brain tissues (Cáceres et al.  
97 2003; Warner et al. 2009; Babbitt et al. 2010) and a small set of other soft tissues (Blekhman et  
98 al. 2008; Karere et al. 2010; Karere et al. 2012; Karere et al. 2013; Tung et al. 2015), have also  
99 noted regulatory differences across species. Methylation differences in brain tissues have  
100 evolved across primates and contributed to resultant brain phenotypes and disease vulnerabilities  
101 (Enard et al. 2004; Kothapalli et al. 2007; Farcas et al. 2009; Provencal et al. 2012; Zeng et al.  
102 2012; Mendizabal et al. 2016; Madrid et al. 2018). Thus, methylation-phenotype relationships  
103 can be identified in primates. Primate methylation patterns in blood cells and other soft tissues  
104 have also been studied, but not to the same degree (Martin et al. 2011; Molaro et al. 2011; Pai et  
105 al. 2011; Fukuda et al. 2013; Hernando-Herraez et al. 2013; Lindskog et al. 2014; Lea et al.  
106 2016; Gao et al. 2017; Vilgalys et al. 2018).

107 Interestingly, two studies using soft tissues and blood identified differential methylation  
108 and expression of genes essential for skeletal development (*RUNX1*, *RUNX3*, and *COL2A1*)  
109 between some primates (Hernando-Herraez et al. 2013; Lindskog et al. 2014). Additionally, the  
110 emerging field of ancient epigenetics, which reconstructs methylation patterns from ancient  
111 DNA degradation patterns in hominin remains (Smith et al. 2015; Gokhman et al. 2014;  
112 Gokhman et al. 2016; Gokhman et al. 2017), have found that other skeletal developmental genes

113 (*HOXD* complex) are differentially methylated among modern humans and ancient hominins  
114 (Gokhman et al. 2014). These findings suggest that primates do exhibit distinct epigenetic  
115 patterns and that the epigenetics of skeletal development may be an important area of research.  
116 Nevertheless, studies of nonhuman primate (NHP) skeletal epigenetics are limited (Housman et  
117 al. 2018).

118 Overall, there are clear knowledge gaps in our understanding of NHP skeletal complexity  
119 in relation to epigenetic variation and epigenetic differences between phylogenetically diverse  
120 NHP species. The present study begins to remedy this by assessing how genome-wide and gene-  
121 specific DNA methylation in primate skeletal tissues varies intra- and inter-specifically and in  
122 relation to femur form. Specifically, for this study, we explored the evolution of the epigenome  
123 and its relation to nonpathological skeletal traits by identifying DNA methylation patterns in  
124 femur trabecular bone from baboons, macaques, vervets, chimpanzees, and marmosets and  
125 assessing intra- and inter-specific methylation variation and its relation to morphology.  
126

## 127 **Results:**

128 The aim of this study was to identify DNA methylation patterns in skeletal tissues from  
129 several NHP species in order to determine how skeletal methylation varies at different taxonomic  
130 scales and in relation to complex skeletal traits. We evaluated DNA methylation patterns in  
131 femur trabecular bone from five NHP species – baboons (n=28), macaques (n=10), vervets  
132 (n=10), chimpanzees (n=4), and marmosets (n=6) (Figure 1, Table S1). We used the Illumina  
133 Infinium MethylationEPIC BeadChip (EPIC array), which was determined to be effective at  
134 identifying DNA methylation patterns in NHP DNA (Supplemental Text, Figures S1-S4, Tables  
135 S2-S5, File S1). Further, we selected probes appropriate for intra- and inter-specific comparison,  
136 which removed the effect of sequence differences among individuals and species as a reason for  
137 methylation differences. With these data, we first tested whether intra-specific variation in  
138 skeletal DNA methylation is associated with intra-specific variation in femur morphology.  
139 Second, we identified inter-specific differences in DNA methylation and assessed whether these  
140 lineage-specific patterns may have contributed to species-specific morphologies.  
141

### 142 ***Genome-Wide Intra-Specific Differential Methylation and Morphological Variation***

143 Measurements of 29 linear morphology traits (Figure 2, Table S6) were collected from  
144 each NHP right femur. All measurements had less than 5% error, except those for intercondylar  
145 notch depth in macaques (Figure S5, File S2). Significant differentially methylated positions  
146 (DMPs) associated with each intra-specific linear morphology were interrogated from 189,858  
147 sites in baboons, 190,898 sites in macaques, 191,639 sites in vervets, 576,804 sites in  
148 chimpanzees, and 68,709 sites in marmosets (Tables S7-S8). In baboons, 1 DMP was  
149 hypomethylated with increasing bicondylar femur length and increasing maximum femur length.  
150 In macaques, 1 DMP was hypermethylated with increasing proximal femur width, 1 DMP was  
151 hypermethylated with increasing medial condyle width, and 6 DMPs were hypomethylated with  
152 increasing medial condyle width. In vervets, 1 DMP was hypomethylated with increasing  
153 superior shaft width, 2 DMPs were hypomethylated with increasing inferior shaft width, and 1  
154 DMP was hypermethylated with increasing anatomical neck height. In chimpanzees, 216 DMPs  
155 were hypomethylated and 57 DMPs were hypermethylated with increasing anatomical neck  
156 length. Lastly, in marmosets, no DMPs were associated with morphological variation (Table S9,  
157 File S3).

158 While the maximum change in mean methylation ( $\Delta\beta$ ) for most of these DMPs is greater  
159 than 10% ( $\Delta\beta = 0.1$ ), the actual  $\Delta\beta$  between individuals with the largest morphology  
160 measurements and individuals with the smallest morphology measurements is less than 0.1 for  
161 several DMPs (File S3). Tests for enrichment of gene ontology (GO) and KEGG pathway  
162 functions were done for the 3 intra-specific morphologies that had more than 2 DMPs associated  
163 with them. However, no GO biological processes were found to be enriched in DMPs associated  
164 with either macaque medial condyle width or chimpanzee anatomical neck length. Additionally,  
165 KEGG pathway functions were only found to be enriched in DMPs associated with chimpanzee  
166 anatomical neck length, and these pathways were predominantly involved in immune system cell  
167 signaling and differentiation (Table S10).

168

### 169 ***Genome-Wide Inter-Specific Differential Methylation***

170 To determine how methylation varies inter-specifically, differential methylation was  
171 interrogated from the 39,802 probes that were shared among NHP species (Table S11, File S4).  
172 Species-specific DMPs were determined by identifying DMPs that were significant in all 4  
173 pairwise comparisons containing the taxon of interest but not in any of the remaining pairwise  
174 comparisons. These methods identified 650 species-specific DMPs in baboons, 257 in macaques,  
175 639 in vervets, 2,796 in chimpanzees, and 13,778 in marmosets (Table S11). Comparably, when  
176 evaluating methylation patterns that distinguish more broad taxonomic groups, 2,701 DMPs  
177 were found to be specific to Old World monkeys (OWMs), 1,439 were found to be ape-specific,  
178 and 15,514 were found to be specific to New World monkeys (NWMs) (File S5). Species-  
179 specific DMPs spanned 7,320 genes (Table S12). While 4,824 of these genes have only a single  
180 probe targeting them, the remaining 2,496 genes contained at least 2 significant probes.  
181 Additionally, these species-specific DMPs covered a range of locations with respect to genes and  
182 CpG islands (Table S12), indicating that these species-specific changes in methylation have a  
183 decent distribution throughout the genome. Using various  $\Delta\beta$  cutoff thresholds decreases the  
184 final number of species-specific DMPs to varying degrees (Table S11, File S4). Counter to these  
185 decreases in numbers, though, species-specific DMPs cover a range of locations with respect to  
186 genes and CpG islands regardless of the  $\Delta\beta$  cutoff threshold (Table S12).

187 Overall, across  $\Delta\beta$  cutoff thresholds, more species-specific DMPs were found in the  
188 NWM marmosets, followed by the great ape chimpanzees, and lastly the OWM baboons,  
189 macaques, and vervets. Additionally, the proportions of hypermethylated and hypomethylated  
190 species-specific DMPs within each taxon remain fairly constant across  $\Delta\beta$  cutoff thresholds  
191 (Table S11). In baboons, macaques, vervets, and chimpanzees, more than half of all species-  
192 specific DMPs show patterns of hypermethylation, and in marmosets, more than half of all  
193 species-specific DMPs show patterns of hypomethylation. The only disruption in these trends is  
194 in chimpanzees when no  $\Delta\beta$  threshold is applied. Nevertheless, species-specific DMPs with  
195 different  $\Delta\beta$  cutoff thresholds do differ in their abilities to cluster animals into taxonomic groups  
196 (Figure S6, File S4). For all thresholds, apes, OWMs, and NWMs cluster into distinct groups.  
197 However, within OWMs, vervets only cluster into a distinct species group with a  $\Delta\beta \geq 0.2$   
198 threshold, and the baboon-macaque clade require a  $\Delta\beta \geq 0.3$  threshold. Lastly, species-specific  
199 clustering of baboons, macaques, and vervets only occurs with a  $\Delta\beta \geq 0.4$  threshold (Figure 3).

200 Additionally, global changes in methylation across all 39,802 probes were evaluated.  
201 Average global changes within each species reveal that apes, OWMs, and NWMs are  
202 phylogenetically distinct from one another, and these divergences are well supported (Figure 4).  
203 Similarly, when phylogenetic relationships are evaluated using the global changes in methylation

204 of individual animals, distinct lineages are again formed between apes, OWMs, and NWMs  
205 (Figure S7). However, within the OWM clade, several poorly supported branches result in  
206 baboons, macaques, and vervets not forming distinct lineages. Phylogenetic separation of these  
207 OWM species into distinct lineages is only possible when the methylation changes considered  
208 are reduced to only include species-specific DMPs with a  $\Delta\beta \geq 0.4$  threshold (Figure S8).

209 Species-specific DMPs also show associations with genes that have a wide array of GO  
210 biological processes (File S6) and KEGG pathway functions (File S7). Cellular adhesion is a  
211 primary GO function found to be highly enriched in species-specific DMPs from macaques,  
212 vervets, chimpanzees, and marmosets. Species-specific DMPs for chimpanzees and marmosets  
213 are also enriched for genes involved in the regulation of transcription and gene expression.  
214 Additionally, enrichment of genes involved in anatomical developmental processes is found in  
215 baboons, chimpanzees, and marmosets. Chimpanzees and marmosets show further enrichment of  
216 genes contributing to pattern specification processes, limb development, and skeletal system  
217 development. Moreover, marmoset species-specific DMPs are enriched for genes with functions  
218 very closely related to skeletal development, such as osteoblast differentiation and ossification,  
219 as well as genes involved in metabolism and the development of other organ systems including  
220 skeletal muscles, nerves, the brain, the heart, blood vessels, kidneys, eyes, and ears (File S6).  
221 Several enriched pathways reinforce these molecular functions, and additional pathways related  
222 to cancers and other disease were also identified (File S7).

223 Out of the species-specific DMPs identified, some were found to overlap with those  
224 previously identified as being differentially methylated among primates. These include *ARTN*,  
225 *COL2A1*, and *GABBR1* which have been found to be differentially methylated among modern  
226 humans and great apes (Hernando-Herraez et al. 2013), as well as *HOXD8*, *HOXD9*, and  
227 *HOXD10* which have been found to be differentially methylated among modern and ancient  
228 hominins (Gokhman et al. 2014). Specifically, 1 marmoset-specific DMP is hypomethylated in  
229 *ARTN*, 3 marmoset-specific DMPs are hypermethylated in *COL2A1*, 2 baboon-specific DMPs  
230 and 3 marmoset-specific DMPs are hypermethylated in *GABBR1*, and 2 marmoset-specific  
231 DMPs are hypomethylated in *GABBR1* (File S4). Additionally, 3 marmoset-specific DMPs are  
232 hypermethylated in *HOXD8*, 1 baboon-specific DMP and 2 marmoset-specific DMPs are  
233 hypermethylated in *HOXD9*, 2 chimpanzee-specific DMPs are hypomethylated in *HOXD9*, and 5  
234 marmoset-specific DMPs are hypermethylated in *HOXD10*. Of these *HOXD10* species-specific  
235 DMPs, 4 have  $\Delta\beta$  between 0.2 and 0.3 and 1 has a  $\Delta\beta < 0.1$  (Figure 5, Table S13).

236

### 237 ***Gene-Specific Inter-Specific DNA Methylation Profiling***

238 Because of the high number of species-specific DMPs within *HOXD10*, methylation  
239 patterns across this gene were assessed at a higher resolution using gene-specific sequencing  
240 techniques. Regular and bisulfite sequences of several regions in the *HOXD10* gene were  
241 generated (Tables S14-S17). First, loci across the entire *HOXD10* gene were examined from a  
242 subset of EPIC array samples – 3 baboons, 3 macaques, 3 vervets, 3 chimpanzees, and 3  
243 marmosets (Figure 6, Tables S1 and S18, File S8-S9). Additionally, one validation locus  
244 (cg02193236) and its surrounding region in *HOXD10* were surveyed in all NHP samples in order  
245 to confirm the reliability of the EPIC array in assessing DNA methylation levels (Figure S9,  
246 Tables S1 and S19, File S10-S11). Overall, regular sequencing was very successful, while  
247 bisulfite sequencing was less successful, with several sequence reads uninterpretable.  
248 Nevertheless, following the alignment of these sequences to the appropriate NHP references, the  
249 presence and absence of methylation across the *HOXD10* gene in each animal was determined

250 (Tables S18-S19, Files S8-S11). These data reveal that across the *HOXD10* gene, NHPs display  
251 generally low methylation with some clustered increased amounts of methylation upstream of the  
252 gene and at the start of the gene body (Figure 6).

253

#### 254 **Discussion:**

255 This study explored skeletal gene regulation and its relation to complex traits and species  
256 differences by evaluating genome-wide and gene-specific DNA methylation patterns in  
257 trabecular bone from several NHP species. These species are phylogenetically representative of  
258 the order and display anatomical and locomotor differences. Specifically, while the sampled  
259 OWMs (baboons, macaques, vervets) display varying levels of terrestrial and arboreal  
260 quadrupedal locomotion, the sampled ape species (chimpanzees) is a knuckle-walking quadruped  
261 that also vertical climbs and occasionally walks bipedally (Cawthon Lang 2006). Even more  
262 distinct are the sampled NWMs (marmosets) which locomote via vertical clinging and leaping  
263 (Cawthon Lang 2005). Lemurs and lorises are the only major taxonomic primate groups not  
264 examined in this study. Regardless, the current sample set provided a unique opportunity to  
265 examine skeletal epigenetic differences in relation to bone morphology. First, we evaluated the  
266 association between intra-specific variation in skeletal DNA methylation and intra-specific  
267 variation in femur morphology. Second, we assessed inter-specific DNA methylation differences  
268 and the potential contribution of these lineage-specific patterns to species-specific morphologies.

269

#### 270 ***Intra-specific DMPs are not readily associated with morphological variants.***

271 With respect to intra-specific morphology, very few sites were found to be differentially  
272 methylated. DMPs were only identified in association with baboon bicondylar femur length,  
273 baboon maximum femur length, macaque proximal femur width, macaque medial condyle width,  
274 vervet superior shaft width, vervet inferior shaft width, vervet anatomical neck height, and  
275 chimpanzee anatomical neck length (Table S8). Additionally, most of these associations only  
276 identified one DMP. This limited number of associations may be due to the small sample sizes  
277 within each species or to the small amount of variation identified in each morphology. This latter  
278 point is supported in that almost all the morphologies with methylation associations also have the  
279 highest intra-specific variation in size (Figure S5, Files S2-S3). Further, because the animals  
280 included in this study were born and raised in captivity, their limited exposure to environmental  
281 variation may limit both the range of phenotypic variation and methylation variation present  
282 within species. Alternatively, it may be the case that DNA methylation variation does not have a  
283 large influence on nonpathological femur morphology within NHPs.

284 Of the few intra-specific methylation patterns associated with morphology, they likely  
285 have weak functional effects. Research has shown that individual site-specific methylation  
286 changes are not readily associated with differential gene expression (Bork et al. 2010; Chen et al.  
287 2011; Koch et al. 2011). Rather, differential gene expression is made possible through the  
288 accumulation of several methylation changes within promotor regions (Suzuki and Bird 2008) or  
289 across the gene body (Singer et al. 2015). Detecting accumulations of methylation changes  
290 across genes should have been possible in the current study as 4-19 probes targeted each gene on  
291 average (Table S4). Thus, the individual sites identified in this study are not due to experimental  
292 limitations and likely have limited impacts on gene regulation. This is further supported by the  
293 degree of methylation variation observed among these DMPs. Sites that have an average change  
294 in mean methylation less than 10% ( $\Delta\beta < 0.1$ ) are thought to have little biological relevance  
295 (Hernando-Herraez et al. 2013). Thus, those DMPs with small changes in methylation likely

296 have little to no biological function. Further, some of the DMPs with  $\Delta\beta \geq 0.1$  appear to be  
297 highly influenced by small subsets of the sample sets. For example, in the case of macaque  
298 proximal width, the majority of methylation change is due to two individuals (1 female and 1  
299 male) that have extremely low methylation at cg19349877 as compared to other macaques (File  
300 S3). Additionally, in the case of chimpanzee anatomical neck length, the 273 DMPs identified  
301 are largely affected by one individual that has a longer anatomical neck than other chimpanzees.  
302 Lastly, the limited enrichment of GO biological processes and KEGG pathway functions among  
303 detected DMPs indicates a lack of common function among these associated regions. Overall,  
304 these finding suggest that while some DMPs appear to be associated with intra-specific  
305 morphological variation in NHPs, not enough evidence is present to support them having a  
306 functional role in the development and maintenance of this morphological variation.

307

### 308 ***Differential methylation is observed among NHP species.***

309 With respect to inter-specific variation, several sites were found to have significant  
310 species-specific methylation differences. Specifically, out of the 39,802 sites examined, 650  
311 species-specific DMPs were identified in baboons, 257 in macaques, 639 in vervets, 2,796 in  
312 chimpanzees, and 13,778 in marmosets, and these span 7,320 genes (Tables S11-S12). However,  
313 many of these DMPs had biologically insignificant changes in mean methylation. Thus, several  
314  $\Delta\beta$  cutoff thresholds were considered – from a 10% change in mean methylation ( $\Delta\beta \geq 0.1$ ) up to  
315 a 40% change in mean methylation ( $\Delta\beta \geq 0.4$ ) – which reduced the overall numbers of species-  
316 specific DMPs. Regardless of  $\Delta\beta$  cutoff threshold, more species-specific DMPs were found in  
317 the NWM marmosets, followed by the great ape chimpanzees, and lastly the OWM baboons,  
318 macaques, and vervets. This trend in numbers of species-specific DMPs is expected given the  
319 known phylogenetic relationships between primates, with OWMs more closely related to apes  
320 and NWMs more distantly related to both groups (Perelman et al. 2011; Rogers and Gibbs 2014).  
321 However, the number of marmoset-specific DMPs is substantially larger than those for other  
322 taxa. While this discrepancy may reflect marmosets having more species-specific changes,  
323 aspects of the experimental design may also contribute to it. Marmosets are the only NWM  
324 included in this study, so although some marmoset-specific DMPs are truly specific to  
325 marmosets, others may be specific to all NWMs. Comparably, OWM-specific DMPs and  
326 catarrhine-specific DMPs may be cancelled out from this study, as such changes would be shared  
327 between all OWMs and catarrhines, respectively. Second, since marmosets are the most  
328 phylogenetically distant from humans as compared to the other NHPs included in this study  
329 (Perelman et al. 2011; Rogers and Gibbs 2014), the probe filtering steps may have biased  
330 downstream data in favor of finding significant results primarily in marmosets. Third, the  
331 marmoset data itself has a slightly different normalized distribution, with more mean methylation  
332 levels of 50%, than that for other NHPs (Figure S4), which may be due to the chimerism often  
333 observed in marmosets. Although, computationally, the filtered array probes examined in this  
334 study appear to hybridize sufficiently for marmosets (Figure S3), there may be other unknown  
335 biological or technical issues that impede proper DNA methylation analyses from the EPIC array  
336 in marmosets and may have inflated the overall number of marmoset-specific DMPs identified.

337 The number of species-specific DMPs identified in this study, is comparable to those  
338 identified in a previous study that assessed methylation patterns in blood from chimpanzees,  
339 bonobos, gorillas, and orangutans using the 450K array and similar alignment criteria filtering  
340 methods with a focus on sites that had a  $\Delta\beta \geq 0.1$  (Hernando-Herraez et al. 2013). This research  
341 used a final set of 99,919 probes that were shared across all great ape species and covered 12,593



342 genes with at least 2 probes per gene. Out of these, 2,284 species-specific DMPs were found in  
343 humans, 1,245 in chimpanzees and bonobos, 1,374 in gorillas, and 5,501 in orangutans  
344 (Hernando-Herraez et al. 2013). In the current study, when a  $\Delta\beta \geq 0.1$  threshold was used, only  
345 1,572 chimpanzee-specific DMPs were identified (Table S11). This number is lower than the  
346 number found in previous research comparing chimpanzees to other great apes (Hernando-  
347 Herraez et al. 2013), species that are evolutionarily closer to chimpanzees than are OWMs and  
348 NWMs (Perelman et al. 2011; Rogers and Gibbs 2014). However, the total number of sites  
349 examined in the present study is approximately one-third of that examined in the prior great ape  
350 study. Thus, a 3-fold increase in the number of sites examined might identify a 3-fold increase in  
351 chimpanzee-specific DMPs as compared to OWMs and NWMs, which would be closer to  
352 expectations (Hernando-Herraez et al. 2013).

353 Additionally, the number of DMPs that distinguish species from one another in the  
354 current study is substantially smaller than the numbers of DMPs identified between different  
355 skeletal tissue types, between different age cohorts, and between individuals with different  
356 skeletal disease states within a NHP species (Housman et al. 2018). This finding is to be  
357 expected since differences in DNA methylation which regulate gene expression (Suzuki and Bird  
358 2008; Singer et al. 2015) should increase or decrease with the degree of differences between  
359 cellular functions among comparative groups (Zhang et al. 2013). In the case of different tissues,  
360 substantial DNA methylation differences likely promote distinct gene regulation that is necessary  
361 for cells in different tissues to promote different functions. In the case of different age cohorts,  
362 slightly fewer DNA methylation differences within the same skeletal tissue may allow cells to  
363 emphasize efforts on growth and development in juveniles, as compared to maintenance in  
364 adults, without altering the general skeletal-related functions of this tissue. In the case of  
365 osteoarthritic disease states, even fewer regulatory changes may be needed to initiate the  
366 dysregulation of tissue function. Finally, the comparatively small number of DNA methylation  
367 differences between adult, skeletally healthy, NHP species seems reasonable given that other  
368 studies have also noted the presence of more regulatory variation within species than between  
369 species (Uebbing et al. 2016). In summary, epigenetic and regulatory differences, which control  
370 and enable age-dependent organ functions, should be greater within a species when comparing  
371 between tissue types, age cohorts, and disease states, than when comparing between species.

372 When evaluating how well the methylation patterns at species-specific DMPs cluster  
373 samples, a  $\Delta\beta \geq 0.4$  threshold is necessary to achieve clustering into distinct species (Figure 3).  
374 Less stringent  $\Delta\beta$  thresholds are able to separate apes, NWMs, and OWMs into distinct groups,  
375 but the OWMs do not form monophyletic species groups at these thresholds (Figure S6). Global  
376 changes in methylation show similar phylogenetic patterns. While average species methylation  
377 patterns reveal a well-supported tree topology that reflects known phylogenetic relationships  
378 between taxa (Perelman et al. 2011; Rogers and Gibbs 2014) (Figure 4), global changes in  
379 methylation among individual animals do not distinguish OWMs into distinct monophyletic  
380 groups (Figure S7). As before, parsing down these global changes to only species-specific DMPs  
381 with  $\Delta\beta \geq 0.4$  fixes the phylogeny (Figure S8). In previous studies, global methylation changes  
382 were able to separate great apes into species-specific phylogenetic groups (Hernando-Herraez et  
383 al. 2013). Conversely, the need for a higher  $\Delta\beta$  cutoff threshold to distinguish species in the  
384 current study may be due to evolutionary reasons.

385 The divergence times between OWMs (baboons, macaques, and vervets) are comparable  
386 to those between great apes (humans, chimpanzees, gorillas, and orangutans) (Perelman et al.  
387 2011). Thus, divergence times do not explain why global changes in methylation are unable to

388 resolve species-specific phylogenetic clades in the current study as compared to previous  
389 research. On the other hand, while nonhuman great apes have experienced higher rates of  
390 molecular evolution as compared to humans (Elango et al. 2006), baboons and macaques have  
391 slow rates of molecular evolution as compared to other OWMs (Elango et al. 2009), which may  
392 correspond to slower rates of epigenetic evolution. This might make baboons and macaques  
393 appear more similar to vervets than expected, and further, this may make resolving the  
394 phylogenetic divergences between OWMs more difficult than that between the great apes.  
395 Additionally, the number of sites included in the present study (39,802) as compared to previous  
396 studies (99,919) (Hernando-Herraez et al. 2013) may limit the ability of the present study to fully  
397 resolve species-specific lineages. This is reinforced by the low support of several branches in the  
398 phylogeny based on global changes in methylation across individual animals (Figure S7).  
399 Conversely, sample size was likely not a contributing factor to the discrepancies between the  
400 current study (n=58) and previous studies (n=32) (Hernando-Herraez et al. 2013), as the current  
401 study has a slightly larger sample size. However, the number of individuals per species was more  
402 uniform in previous studies (Hernando-Herraez et al. 2013) than in the current study.

403 Alternatively, the fact that global changes in methylation are unable to fully resolve  
404 OWM species-specific phylogenetic clades in the current study, may instead indicate that not  
405 enough time has passed for OWM species to evolve fixed epigenetic changes between taxa in  
406 this tissue. Additionally, it is possible that epigenetic variation at many of the sites examined in  
407 this study are under balancing selection in OWMs which prevents these markers from accurately  
408 resolving the evolutionary divergences between these species. However, previous research of  
409 gene regulation differences between species has found that while some drastic deviations in gene  
410 expression may be under directional or balancing selection (Whitehead and Crawford 2006;  
411 Romero et al. 2012), most inter-specific regulatory differences appear to be under stabilizing  
412 selection or neutral evolution (Brawand et al. 2011; Gilad 2012; Romero et al. 2012).

413

#### 414 ***Inter-specific DMPs are found in genes enriched for functions associated with skeletal traits.***

415 The evolution of methylation changes along specific NHP lineages is associated with  
416 several functions that may contribute to species-specific phenotypic differences (Files S6-S7).  
417 First, several skeletal tissue functions are enriched in species-specific DMPs. Among almost all  
418 NHPs, cellular adhesion functions are highly enriched. Cellular adhesion is necessary for cells to  
419 attach to other cells or extracellular matrix, which is a necessity for bone cells (Mbalaviele et al.  
420 2006). Additionally, in baboons, chimpanzees, and marmosets, anatomical developmental  
421 processes are enriched, and in chimpanzees and marmosets, pattern specification processes, limb  
422 development, and skeletal system development are enriched. Lastly, in marmosets, specific  
423 skeletal functions, such as osteoblast differentiation and ossification are also enriched. Overall,  
424 these functions validate that most patterns of differential methylation relate to skeletal tissue  
425 function, regulation, development, and maintenance, as well to larger anatomical developmental  
426 processes. Additionally, functions not specific to the skeletal system were identified. In  
427 chimpanzees and marmosets, transcription and gene expression regulatory functions were  
428 enriched. Further, in marmosets, functions related to the development of skeletal muscles,  
429 nerves, the brain, the heart, blood vessels, kidneys, eyes, and ears were also enriched. All  
430 together, these findings suggest that many species-specific changes in methylation may  
431 contribute to the regulation of complex phenotypic changes. While this relationship was not  
432 observed for intra-specific skeletal morphology variation, other skeletal traits not examined in  
433 this study may be related. Nevertheless, many of the genes associated with the described

434 functions only contain an average of 1-2 differentially methylated sites. As described above,  
435 individual site-specific methylation changes are not readily associated with differential gene  
436 expression (Bork et al. 2010; Chen et al. 2011; Koch et al. 2011). Therefore, the enriched  
437 functions identified are likely not true biological effects due to methylation differences on their  
438 own. Rather they hint at biological effects that may be the result of the combined effects of  
439 several genetic, epigenetic, and other regulatory processes.

440 Finally, some of the genes containing species-specific DMPs overlap with those  
441 previously identified as being differentially methylated in other tissues among primates.  
442 Specifically, the neurotrophic factor *ARTN* shows species-specific hypomethylation at 1 site in  
443 marmosets, and in previous work it shows species-specific hypermethylation at 3 sites in humans  
444 as compared to other great apes (Hernando-Herraez et al. 2013). Additionally, *COL2A1* which  
445 codes for the predominant type of collagen in cartilage, shows species-specific hypermethylation  
446 at 3 sites in marmosets, and in previous work it shows species-specific hypermethylation of 4  
447 sites in humans as compared to other great apes (Hernando-Herraez et al. 2013). The neuronal  
448 receptor *GABBR1* shows more complicated methylation patterns. In the current study, *GABBR1*  
449 shows species-specific hypermethylation at 2 sites in baboons, hypermethylation at 3 sites in  
450 marmosets, and hypomethylation at 2 sites in marmosets. In previous work, *GABBR1* shows  
451 hypomethylation in orangutans and hypermethylation in chimpanzees and bonobos (Hernando-  
452 Herraez et al. 2013). Lastly, 3 genes within the *HOXD* cluster, which are involved in limb  
453 development, also show complicated methylation patterns. In the current study, *HOXD8* shows  
454 species-specific hypermethylation at 3 sites in marmoset, *HOXD9* shows species-specific  
455 hypermethylation at 1 site in baboons and 2 sites in marmosets and species-specific  
456 hypomethylation at 2 sites in chimpanzees, and *HOXD10* shows species-specific  
457 hypermethylation at 5 sites in marmosets. In previous work, *HOXD8* shows hypomethylation in  
458 modern and archaic hominins while *HOXD9* and *HOXD10* show hypermethylation in archaic  
459 hominins as compared to modern humans (Gokhman et al. 2014).

460 In the *HOXD* cluster, *HOXD10* contains the largest number of NHP species-specific  
461 methylation differences observed in this study, has an active role in anatomical development, and  
462 has been found to be differentially methylated among hominins. Thus, it was selected for  
463 subsequent DNA methylation profiling and analysis at a higher resolution using gene-specific  
464 sequencing techniques. *HOXD10* specifically codes for a protein that functions as a sequence-  
465 specific transcription factor which is expressed in the developing limb buds and is involved in  
466 differentiation and limb development. In the current study, each NHP shows low to intermediate  
467 methylation levels across the gene body (Figure 5, Table S13). A similar pattern is observed in  
468 the gene-specific methylation data, which further reveals that *HOXD10* is not highly methylated  
469 in NHPs. However, across all taxa, some clusters of hypermethylation are found upstream of the  
470 gene and at the start of the gene body, with marmosets on average displaying more methylation  
471 in the gene body than other taxa (Figure 6, Table S18). In the *HOXD10* gene body of hominins,  
472 humans display hypomethylation, Neandertals displayed intermediate methylation levels, and  
473 Denisovans displayed high levels of methylation (Gokhman et al. 2014). The variation of  
474 methylation patterns in this gene body suggest that intermediate methylation levels may be a  
475 more ancestral epigenetic state for this region in the primate lineage, while the extreme  
476 hypermethylation of this region in Denisovans and the extreme hypomethylation of this region in  
477 humans may be derived epigenetic states. Previous work has proposed that methylation  
478 differences in *HOXD10* may be associated with phenotypic distinctions between modern human  
479 and archaic hominin limbs (Gokhman et al. 2014). While the current study did not find

480 substantial associations between methylation variation and aspects of femur morphology within  
481 NHP species, further work to understand the role of differential methylation of *HOXD10* in  
482 promoting morphological changes of the limb should be explored.

483 In conclusion, while only a few significant associations were identified between  
484 methylation and femur morphologies, several significant differences in methylation were  
485 observed inter-specifically. Moreover, these species-specific DMPs were found in genes  
486 enriched for functions associated with complex skeletal traits. This is the first study to  
487 characterize DNA methylation patterns in skeletal tissues from a taxonomically diverse set of  
488 NHPs, and it is the first study to directly compare these patterns to the nonpathological  
489 morphologies of the skeletal elements from which the tissues were derived. This design enabled  
490 an initial exploration of skeletal gene regulation and its relation to complex traits and species  
491 differences for which little else is currently known.

492

## 493 **Materials and Methods:**

494

### 495 *Ethics Statement*

496 NHP tissue samples included were opportunistically collected at routine necropsy of these  
497 animals. No animals were sacrificed for this study, and no living animals were used in this study.  
498 Chimpanzee tissues were collected opportunistically during routine necropsy prior to the  
499 September 2015 implementation of Fish and Wildlife Service rule 80 FR 34499.

500

### 501 *NHP Samples*

502 NHP samples come from captive colonies of chimpanzees (*Pan troglodytes*), baboons  
503 (*Papio spp.*), rhesus macaques (*Macaca mulatta*), and marmosets (*Callithrix jacchus*) from the  
504 Southwest National Primate Research Center in Texas, as well as vervets (*Chlorocebus aethiops*)  
505 from the Wake Forest/UCLA Vervet Research Colony in North Carolina. Femora were  
506 opportunistically collected at routine necropsy of these animals and stored in -20°C freezers at  
507 the Texas Biomedical Research Institute after dissection. These preparation and storage  
508 conditions ensured the preservation of skeletal DNA methylation patterns. Samples include  
509 baboons (n=28), macaques (n=10), vervets (n=10), chimpanzees (n=4), and marmosets (n=6).  
510 Age ranges span adulthood for each species and are comparable between each group (Figure 1,  
511 Table S1). Both sexes are represented (female: n=33, male: n=24, unknown: n=1).

512

### 513 *Assessment of Femur Morphologies*

514 On the right femora of NHP samples, 29 linear morphology traits (Figure 2, Table S6)  
515 were measured using calipers. These measurements characterize overall femur shape (McHenry  
516 and Corruccini 1978; Terzidis et al. 2012). Error for each measurement was determined by  
517 performing triplicate measurements on approximately 10% of the samples in each species. These  
518 measurements were spaced throughout the entire data collection period. Error was calculated as  
519 the mean absolute difference divided by the mean (Corner et al. 1992; White and Folkens 2000).  
520 All measurements that were retained for downstream analyses had errors of less than 5%, and the  
521 only measurement excluded was macaque intercondylar notch depth (error = 6.62%) (File S2).

522

### 523 *Genome-Wide DNA Methylation Profiling*

524 Trabecular bone cores were obtained from the medial condyles on the right distal femora  
525 of each NHP sample using a drill press that cored transversely through the condyle leaving the

526 articular surface preserved. Cortical bone was removed from cores using a Dremel, and the  
527 remaining trabecular bone cores were pulverized into bone dust using a SPEX SamplePrep  
528 Freezer/Mill. DNA was extracted from femoral trabecular bone using a phenol-chloroform  
529 protocol optimized for skeletal tissues (Barnett and Larson 2012). Genome-wide DNA  
530 methylation was assessed using Illumina Infinium MethylationEPIC microarrays (EPIC array)  
531 (Supplemental Text). The array data discussed in this publication have been deposited in NCBI's  
532 Gene Expression Omnibus and are accessible through GEO SuperSeries accession number  
533 GSE103332, which includes the SubSeries accession numbers GSE103279, GSE103271,  
534 GSE103280, GSE94677, GSE103328, and GSE103287.

535

### 536 ***Methylation Data Processing***

537 Using previously described methods (Housman et al. 2018), raw EPIC array data were  
538 normalized and converted to  $\beta$  values which represent the average methylation levels at each site  
539 (0 = completely unmethylated sites, 1 = fully methylated sites), and M values which are the log  
540 transformed ratio of methylated signal to unmethylated signal. Probes with failed detection levels  
541 ( $p$ -value  $> 0.05$ ) in greater than 10% of samples and samples with greater than 30% of probes  
542 with detection level failures were removed from downstream analyses. Using previously  
543 described methods (Housman et al. 2018), probes with sequence mismatches to NHP genomes,  
544 which could produce biased methylation measurements, were computationally filtered out and  
545 excluded from downstream analyses (Supplemental Text, Figures S1-S3, Tables S2-S5, File S1).  
546 Additionally, cross-reactive probes (McCartney et al. 2016), probes containing SNPs at the CpG  
547 site, probes detecting SNP information, probes detecting methylation at non-CpG sites, and  
548 probes targeting sites within the sex chromosomes were removed (Aryee et al. 2014; Fortin et al.  
549 2016). This resulted in finalized datasets (Figure S4) that were used in further statistical analyses.

550

### 551 ***Statistical Analysis of Differential Methylation***

552 In order to identify sites that were significantly differentially methylated across  
553 comparative groups, we designed and tested generalized linear mixed models (GLMMs) which  
554 related the variables of interest (morphological measures and species membership) to the DNA  
555 methylation patterns for each site, while accounting for the effects of additional variables, batch  
556 effects, and latent variables (Maksimovic et al. 2016). Sites found to have significant  
557 associations were classified as significant differentially methylated positions (DMPs).  
558 Specifically, a GLMM was used to estimate differences in methylation levels associated with the  
559 femur morphology within each taxonomic group (intra-specific) and between each taxonomic  
560 group (inter-specific) (Supplemental Text).

561

### 562 ***Intra-Specific Analyses***

563 For the intra-specific analyses, variables included in each GLMM were the femur  
564 morphologies within each taxonomic group, sex, age, and steady state weight when known, as  
565 well as unknown latent variables calculated using the iteratively re-weighted least squares  
566 approach in the *sva* package in R (Leek and Storey 2007; Leek and Storey 2008; Leek et al.  
567 2012; Jaffe and Irizarry 2014). Latent variables estimated for each morphology were included to  
568 help mitigate any unknown batch and cell heterogeneity effects on methylation variation at each  
569 site (Table S7). Each GLMM design matrix was fit to corresponding M value array data by  
570 generalized least squares using the *limma* package in R (Huber et al. 2015; Ritchie et al. 2015;  
571 Phipson et al. 2016), and the estimated coefficients and standard errors for each morphology

572 were computed. Lastly, for each coefficient, an empirical Bayes approach (Lönstedt and Speed  
573 2002; Smyth 2004; McCarthy and Smyth 2009; Phipson et al. 2016) was used to compute  
574 moderated t-statistics, log-odds ratios of differential methylation, and associated p-values  
575 adjusted for multiple testing (Benjamini and Hochberg 1995). Significant DMPs for the effect of  
576 each morphology were defined as those having log fold changes in M values corresponding to an  
577 adjusted p-value of less than 0.05. Lastly, the gene ontology (GO) and KEGG pathway  
578 enrichment for significant CpGs was determined using the missMethyl package in R (Benjamini  
579 and Hochberg 1995; Young et al. 2010; Gleeher et al. 2013; Ritchie et al. 2015), which takes  
580 into account the differing number of probes per gene present on the array.

581

### 582 *Inter-Specific Analyses*

583 For the inter-specific analyses, variables included in the GLMM were taxonomic  
584 grouping, sex, age, known batch effects (e.g., array number and position), and unknown latent  
585 variables calculated using the method described above. The four latent variables estimated were  
586 included to help mitigate any unknown batch and cell heterogeneity effects on methylation  
587 variation at each site. The GLMM design matrix was fit to the M value array data using the  
588 method described above, and the estimated coefficients and standard errors for taxonomic group  
589 effects were computed. As described above, moderated t-statistics, log-odds ratios of differential  
590 methylation, and associated p-values adjusted for multiple testing were computed, and  
591 significant DMPs for the effect of taxonomy were defined as those having log fold changes in M  
592 values corresponding to an adjusted p-value of less than 0.05.

593 To determine only those methylation differences that represent fixed changes between  
594 genera, we used methods similar to those described in (Hernando-Herraez et al. 2013). Briefly,  
595 significant DMPs were identified between all possible pairwise comparisons of taxa (n=10:  
596 baboon-macaque, baboon-vervet, baboon-chimpanzee, baboon-marmoset, macaque-vervet,  
597 macaque-chimpanzee, macaque-marmoset, vervet-chimpanzee, vervet-marmoset, chimpanzee-  
598 marmoset). A significant DMP was then defined as taxon-specific if it was found to be  
599 significant in all four pairwise comparisons containing the taxon of interest but not found in any  
600 of the remaining pairwise comparisons. The GO and KEGG pathway enrichment of these DMPs  
601 was then determined as described above.

602 Additionally, global changes in methylation were calculated using distance matrices  
603 (Hernando-Herraez et al. 2013) of the methylation levels for all finalized 39,802 filtered probes.  
604 These changes were assessed at a species-level by averaging the  $\beta$  values per probe within each  
605 species. We then used Euclidean distances to calculate the difference between every two species.  
606 Neighbor joining trees were estimated from these distances using the ape package in R (Paradis  
607 et al. 2004). For each resulting tree, 1000 bootstraps were performed to determine confidence  
608 values for each branch. Global changes in methylation were also assessed at the individual-level  
609 using Euclidean distances to calculate the difference between every two individuals.

610

### 611 *Gene-Specific DNA Methylation Profiling and Analyses*

612 Based on the inter-specific DNA methylation patterns identified in this study and those  
613 identified in other evolutionary anthropological studies (Gokhman et al. 2014), the *HOXD10*  
614 gene was selected for subsequent DNA methylation profiling and analysis at a higher resolution  
615 using gene-specific sequencing techniques. Specifically, primers were designed and optimized to  
616 PCR amplify regions spanning across the entire *HOXD10* gene, as well as upstream and  
617 downstream several hundred bases (hg19 chr2:176980532-176985117), in each NHP species for

618 regular and bisulfite treated DNA (Tables S14-S17). All gene-specific assays were performed in  
619 a subset of the samples tested using the EPIC array and included chimpanzees (n=3), baboons  
620 (n=3), macaques (n=3), vervets (n=3), and marmosets (n=3) (Table S1). Additionally, a subset of  
621 these assays that targeted one validation locus (cg02193236) were performed in all of the  
622 samples (Table S1). As described above, DNA was extracted from femoral trabecular bone using  
623 a phenol-chloroform protocol optimized for skeletal tissues (Barnett and Larson 2012). DNA  
624 was bisulfite converted using the EZ DNA Methylation™ Gold Kit according to the  
625 manufacturer's instructions (Zymo Research). Successful PCR amplification was confirmed  
626 using gel electrophoresis. Gene-specific PCR products were then purified using an exonuclease I  
627 and shrimp alkaline phosphatase protocol and sequenced on the Applied Biosystems 3730  
628 capillary sequencer at the DNA Laboratory at Arizona State University.

629 Regular and bisulfite sequences were aligned to the appropriate NHP references within  
630 the Enredo-Pecan-Orthus (EPO) whole-genome multiple alignments of several primate genomes  
631 [Ensembl Compara.8\_primates\_EPO] (Paten, Herrero, Beal, et al. 2008; Paten, Herrero,  
632 Fitzgerald, et al. 2008) using MEGA7 (Kumar et al. 2016). Manual annotation of these  
633 sequences within each sample confirmed that the gene sequences belong to the appropriate  
634 primate species and that the regular and bisulfite treated sequences only differ in cytosine  
635 composition. The number and distribution of methylated loci throughout the *HOXD10* gene were  
636 then identified compared within and among species to provide a higher resolution of methylation  
637 variation within this targeted gene. Lastly, with respect to the validation locus (cg02193236)  
638 evaluated in all samples, methylation levels across this region were confirmed to correspond with  
639 the methylation levels of this region as determined using the EPIC array.

640

#### 641 **Acknowledgements and Funding Information:**

642 This work was supported by the National Institutes of Health (P01 HL028972 to Anthony  
643 G. Comuzzie); the Leakey Foundation (Research Grant for Doctoral Students to G.H.); the  
644 Wenner-Gren Foundation (Gr. 9310 to G.H.); the Nacey Maggioncalda Foundation (James F.  
645 Nacey Fellowship to G.H.); the International Primatological Society (to G.H.); Sigma Xi (Grant-  
646 in-Aid of Research to G.H.); the ASU Center for Evolution and Medicine (Venture Fund to  
647 G.H.); the ASU Graduate Research and Support Program (to G.H.). Additionally, this  
648 investigation used resources that were supported by the Southwest National Primate Research  
649 Center grant P51 OD011133 from the Office of Research Infrastructure Programs, National  
650 Institutes of Health.

651 We thank Eric D. Johnson and members of the Department of Genetics at the Texas  
652 Biomedical Research Institute, including Anthony G. Comuzzie, Anne Sheldrake, Jaydee Foster,  
653 Kara Peterson, Mel Carless, and Laura Cox, for helpful discussions. We also thank Megann  
654 Phillips for assistance with PCR primer design.

655 Newly reported data have been made available on NCBI's Gene Expression Omnibus and  
656 are accessible through the GEO SuperSeries accession number GSE103332, which includes the  
657 following SubSeries accession numbers: GSE103279 (intra-specific baboon DNA methylation  
658 data), GSE103271 (intra-specific macaque DNA methylation data), GSE103280 (intra-specific  
659 vervet DNA methylation data), GSE94677 (intra-specific chimp DNA methylation data),  
660 GSE103328 (intra-specific marmoset DNA methylation data), and GSE103287 (inter-specific  
661 DNA methylation data).

662

#### 663 **References:**

- 664 de Andrés MC, Kingham E, Imagawa K, Gonzalez A, Roach HI, Wilson DI, Oreffo ROC. 2013.  
665 Epigenetic Regulation during Fetal Femur Development: DNA Methylation  
666 Matters. Neves NM, editor. PLoS ONE 8:e54957.
- 667 Ankel-Simons F. 2007. Primate Anatomy. 3rd ed. New York: Academic Press
- 668 Aryee MJ, Jaffe AE, Corrada-Bravo H, Ladd-Acosta C, Feinberg AP, Hansen KD, Irizarry RA.  
669 2014. Minfi: a flexible and comprehensive Bioconductor package for the analysis of  
670 Infinium DNA methylation microarrays. Bioinformatics 30:1363–1369.
- 671 Babbitt CC, Fedrigo O, Pfefferle AD, Boyle AP, Horvath JE, Furey TS, Wray GA. 2010. Both  
672 Noncoding and Protein-Coding RNAs Contribute to Gene Expression Evolution in the  
673 Primate Brain. Genome Biol. Evol. 2:67–79.
- 674 Bell CG, Wilson GA, Butcher LM, Roos C, Walter L, Beck S. 2012. Human-specific CpG  
675 “beacons” identify loci associated with human-specific traits and disease. Epigenetics  
676 7:1188–1199.
- 677 Benjamini Y, Hochberg Y. 1995. Controlling the False Discovery Rate: A Practical and  
678 Powerful Approach to Multiple Testing. J. R. Stat. Soc. Ser. B Methodol. 57:289–300.
- 679 Blekhman R, Oshlack A, Chabot AE, Smyth GK, Gilad Y. 2008. Gene Regulation in Primates  
680 Evolves under Tissue-Specific Selection Pressures. McVean G, editor. PLoS Genet.  
681 4:e1000271.
- 682 Bork S, Pfister S, Witt H, Horn P, Korn B, Ho AD, Wagner W. 2010. DNA methylation pattern  
683 changes upon long-term culture and aging of human mesenchymal stromal cells. Aging  
684 Cell 9:54–63.
- 685 Bovée JVMG, Hogendoorn PCW, Wunder JS, Alman BA. 2010. Cartilage tumours and bone  
686 development: molecular pathology and possible therapeutic targets. Nat. Rev. Cancer  
687 10:481–488.
- 688 Brand-Saberi B. 2005. Genetic and epigenetic control of skeletal muscle development. Ann.  
689 Anat. - Anat. Anz. 187:199–207.
- 690 Brawand D, Soumillon M, Necsulea A, Julien P, Csárdi G, Harrigan P, Weier M, Liechti A,  
691 Aximu-Petri A, Kircher M, et al. 2011. The evolution of gene expression levels in  
692 mammalian organs. Nature 478:343–348.
- 693 Cáceres M, Lachuer J, Zapala MA, Redmond JC, Kudo L, Geschwind DH, Lockhart DJ, Preuss  
694 TM, Barlow C. 2003. Elevated gene expression levels distinguish human from non-  
695 human primate brains. Proc. Natl. Acad. Sci. 100:13030–13035.
- 696 Cawthon Lang KA. 2005. Primate Factsheets: Common marmoset (*Callithrix jacchus*)  
697 Taxonomy, Morphology, & Ecology. Available from:  
698 [http://pin.primate.wisc.edu/factsheets/entry/common\\_marmoset](http://pin.primate.wisc.edu/factsheets/entry/common_marmoset)
- 699 Cawthon Lang KA. 2006. Primate Factsheets: Chimpanzee (*Pan troglodytes*) Taxonomy,  
700 Morphology, & Ecology. Available from:  
701 <http://pin.primate.wisc.edu/factsheets/entry/chimpanzee>
- 702 Chen Y, Choufani S, Ferreira JC, Grafodatskaya D, Butcher DT, Weksberg R. 2011. Sequence  
703 overlap between autosomal and sex-linked probes on the Illumina HumanMethylation27  
704 microarray. Genomics 97:214–222.
- 705 Corner B, Lele S, Richtsmeier J. 1992. Measuring precision of three-dimensional landmark data.  
706 J. Quant. Anthropol. 3:347–359.
- 707 Delgado-Calle J, Fernández AF, Sainz J, Zarrabeitia MT, Sañudo C, García-Renedo R, Pérez-  
708 Núñez MI, García-Ibarbia C, Fraga MF, Riancho JA. 2013. Genome-wide profiling of



- 709 bone reveals differentially methylated regions in osteoporosis and osteoarthritis. *Arthritis*  
710 *Rheum.* 65:197–205.
- 711 Dimitriou R, Jones E, McGonagle D, Giannoudis PV. 2011. Bone regeneration: current concepts  
712 and future directions. *BMC Med.* 9:1.
- 713 van Dongen J, Ehli E, Sliker R, Bartels M, Weber Z, Davies G, Slagboom P, Heijmans B,  
714 Boomsma D. 2014. Epigenetic Variation in Monozygotic Twins: A Genome-Wide  
715 Analysis of DNA Methylation in Buccal Cells. *Genes* 5:347–365.
- 716 Elango N, Lee J, Peng Z, Loh Y-HE, Yi SV. 2009. Evolutionary rate variation in Old World  
717 monkeys. *Biol. Lett.* 5:405–408.
- 718 Elango N, Thomas JW, Program†§ NCS, Yi SV. 2006. Variable molecular clocks in hominoids.  
719 *Proc. Natl. Acad. Sci.* 103:1370–1375.
- 720 Enard W, Fassbender A, Model F, Adorján P, Pääbo S, Olek A. 2004. Differences in DNA  
721 methylation patterns between humans and chimpanzees. *Curr. Biol.* 14:R148–R149.
- 722 Farcas R, Schneider E, Frauenknecht K, Kondova I, Bontrop R, Bohl J, Navarro B, Metzler M,  
723 Zischler H, Zechner U, et al. 2009. Differences in DNA Methylation Patterns and  
724 Expression of the CCRK Gene in Human and Nonhuman Primate Cortices. *Mol. Biol.*  
725 *Evol.* 26:1379–1389.
- 726 Fernández-Tajes J, Soto-Hermida A, Vázquez-Mosquera ME, Cortés-Pereira E, Mosquera A,  
727 Fernández-Moreno M, Oreiro N, Fernández-López C, Fernández JL, Rego-Pérez I, et al.  
728 2014. Genome-wide DNA methylation analysis of articular chondrocytes reveals a  
729 cluster of osteoarthritic patients. *Ann. Rheum. Dis.* 73:668–677.
- 730 Flanagan JM, Pependikyte V, Pozdniakovaite N, Sobolev M, Assadzadeh A, Schumacher A,  
731 Zangeneh M, Lau L, Virtanen C, Wang S-C, et al. 2006. Intra- and Interindividual  
732 Epigenetic Variation in Human Germ Cells. *Am. J. Hum. Genet.* 79:67–84.
- 733 Fleagle JG. 1999. *Primate Adaptation and Evolution.* New York: Academic Press
- 734 Fortin J-P, Triche T, Hansen K. 2016. Preprocessing, normalization and integration of the  
735 Illumina HumanMethylationEPIC array. *bioRxiv:065490.*
- 736 Fraga MF, Ballestar E, Paz MF, Ropero S, Setien F, Ballestar ML, Heine-Suñer D, Cigudosa JC,  
737 Urioste M, Benitez J, et al. 2005. Epigenetic differences arise during the lifetime of  
738 monozygotic twins. *Proc. Natl. Acad. Sci. U. S. A.* 102:10604–10609.
- 739 Fukuda K, Ichiyanagi K, Yamada Y, Go Y, Udono T, Wada S, Maeda T, Soejima H, Saitou N,  
740 Ito T, et al. 2013. Regional DNA methylation differences between humans and  
741 chimpanzees are associated with genetic changes, transcriptional divergence and disease  
742 genes. *J. Hum. Genet.* 58:446–454.
- 743 Gama-Sosa MA, Midgett RM, Slagel VA, Githens S, Kuo KC, Gehrke CW, Ehrlich M. 1983.  
744 Tissue-specific differences in DNA methylation in various mammals. *Biochim. Biophys.*  
745 *Acta BBA-Gene Struct. Expr.* 740:212–219.
- 746 Gao F, Niu Y, Sun YE, Lu H, Chen Y, Li S, Kang Y, Luo Y, Si C, Yu J, et al. 2017. De novo  
747 DNA methylation during monkey pre-implantation embryogenesis. *Cell Res.* [Internet].  
748 Available from: <http://www.nature.com/cr/journal/vaop/ncurrent/full/cr201725a.html>
- 749 García-Ibarbia C, Delgado-Calle J, Casafont I, Velasco J, Arozamena J, Pérez-Núñez MI, Alonso  
750 MA, Berciano MT, Ortiz F, Pérez-Castrillón JL, et al. 2013. Contribution of genetic and  
751 epigenetic mechanisms to Wnt pathway activity in prevalent skeletal disorders. *Gene*  
752 532:165–172.

- 753 Geeleher P, Hartnett L, Egan LJ, Golden A, Raja Ali RA, Seoighe C. 2013. Gene-set analysis is  
754 severely biased when applied to genome-wide methylation data. *Bioinforma. Oxf. Engl.*  
755 29:1851–1857.
- 756 Gibbs JR, van der Brug MP, Hernandez DG, Traynor BJ, Nalls MA, Lai S-L, Arepalli S,  
757 Dillman A, Rafferty IP, Troncoso J, et al. 2010. Abundant Quantitative Trait Loci Exist  
758 for DNA Methylation and Gene Expression in Human Brain. Flint J, editor. *PLoS Genet.*  
759 6:e1000952.
- 760 Gilad Y. 2012. Using Genomic Tools to Study Regulatory Evolution. *Methods Mol. Biol. Clifton*  
761 *NJ* 856:335–361.
- 762 Gokhman D, Agranat-Tamir L, Housman G, Garcia-Perez R, Nissim-Rafinia M, Mallick S,  
763 Nieves-Colón M, Li H, Alpaslan-Roodenberg S, Novak M, et al. 2017. Extensive  
764 Regulatory Changes in Genes Affecting Vocal and Facial Anatomy Separate Modern  
765 from Archaic Humans. *bioRxiv:106955*.
- 766 Gokhman D, Lavi E, Prüfer K, Fraga MF, Riancho JA, Kelso J, Pääbo S, Meshorer E, Carmel L.  
767 2014. Reconstructing the DNA methylation maps of the Neandertal and the Denisovan.  
768 *Science* 344:523–527.
- 769 Gokhman D, Meshorer E, Carmel L. 2016. Epigenetics: It’s Getting Old. Past Meets Future in  
770 Paleoeugenetics. *Trends Ecol. Evol.* 31:290–300.
- 771 Goldring MB, Marcu KB. 2012. Epigenomic and microRNA-mediated regulation in cartilage  
772 development, homeostasis, and osteoarthritis. *Trends Mol. Med.* 18:109–118.
- 773 Haygood R, Fedrigo O, Hanson B, Yokoyama K-D, Wray GA. 2007. Promoter regions of many  
774 neural- and nutrition-related genes have experienced positive selection during human  
775 evolution. *Nat. Genet.* 39:1140–1144.
- 776 Henriksen M, Creaby MW, Lund H, Juhl C, Christensen R. 2014. Is there a causal link between  
777 knee loading and knee osteoarthritis progression? A systematic review and meta-analysis  
778 of cohort studies and randomised trials. *BMJ Open* 4:e005368.
- 779 Hernando-Herraez I, Prado-Martinez J, Garg P, Fernandez-Callejo M, Heyn H, Hvilsom C,  
780 Navarro A, Esteller M, Sharp AJ, Marques-Bonet T. 2013. Dynamics of DNA  
781 Methylation in Recent Human and Great Ape Evolution. *PLOS Genet* 9:e1003763.
- 782 Heyn H, Moran S, Hernando-Herraez I, Sayols S, Gomez A, Sandoval J, Monk D, Hata K,  
783 Marques-Bonet T, Wang L, et al. 2013. DNA methylation contributes to natural human  
784 variation. *Genome Res.* 23:1363–1372.
- 785 den Hollander W, Ramos YFM, Bos SD, Bomer N, van der Breggen R, Lakenberg N, de Dijcker  
786 WJ, Duijnisveld BJ, Slagboom PE, Nelissen RGHH, et al. 2014. Knee and hip articular  
787 cartilage have distinct epigenomic landscapes: implications for future cartilage  
788 regeneration approaches. *Ann. Rheum. Dis.* 73:2208–2212.
- 789 Housman G, Havill LM, Quillen EE, Comuzzie AG, Stone AC. 2018. Assessment of DNA  
790 Methylation Patterns in the Bone and Cartilage of a Nonhuman Primate Model of  
791 Osteoarthritis. *CARTILAGE* [Internet]. Available from:  
792 <http://journals.sagepub.com/eprint/UzBEFuVaATyPnanB3shB/full>
- 793 Huber W, Carey VJ, Gentleman R, Anders S, Carlson M, Carvalho BS, Bravo HC, Davis S,  
794 Gatto L, Girke T, et al. 2015. Orchestrating high-throughput genomic analysis with  
795 Bioconductor. *Nat. Methods* 12:115–121.
- 796 Iliopoulos D, Malizos KN, Oikonomou P, Tsezou A. 2008. Integrative MicroRNA and  
797 Proteomic Approaches Identify Novel Osteoarthritis Genes and Their Collaborative  
798 Metabolic and Inflammatory Networks. Koutsopoulos S, editor. *PLoS ONE* 3:e3740.

- 799 Jacob RA, Gretz DM, Taylor PC, James SJ, Pogribny IP, Miller BJ, Henning SM, Swendseid  
800 ME. 1998. Moderate folate depletion increases plasma homocysteine and decreases  
801 lymphocyte DNA methylation in postmenopausal women. *J. Nutr.* 128:1204–1212.
- 802 Jaffe AE, Irizarry RA. 2014. Accounting for cellular heterogeneity is critical in epigenome-wide  
803 association studies. *Genome Biol.* 15:R31.
- 804 Jeffries MA, Donica M, Baker LW, Stevenson ME, Annan AC, Beth Humphrey M, James JA,  
805 Sawalha AH. 2016. Genome-Wide DNA Methylation Study Identifies Significant  
806 Epigenomic Changes in Osteoarthritic Subchondral Bone and Similarity to Overlying  
807 Cartilage. *Arthritis Rheumatol.* 68:1403–1414.
- 808 Jeffries MA, Donica M, Baker LW, Stevenson ME, Annan AC, Humphrey MB, James JA,  
809 Sawalha AH. 2014. Genome-Wide DNA Methylation Study Identifies Significant  
810 Epigenomic Changes in Osteoarthritic Cartilage. *Arthritis Rheumatol.* 66:2804–2815.
- 811 Joganic JL, Willmore KE, Richtsmeier JT, Weiss KM, Mahaney MC, Rogers J, Cheverud JM.  
812 2017. Additive genetic variation in the craniofacial skeleton of baboons (genus *Papio*)  
813 and its relationship to body and cranial size. *Am. J. Phys. Anthropol.*:1–17.
- 814 Karere GM, Glenn JP, Birnbaum S, Rainwater DL, Mahaney MC, VandeBerg JL, Cox LA.  
815 2013. Identification of candidate genes encoding an LDL-C QTL in baboons. *J. Lipid*  
816 *Res.* 54:1776–1785.
- 817 Karere GM, Glenn JP, VandeBerg JL, Cox LA. 2010. Identification of baboon microRNAs  
818 expressed in liver and lymphocytes. *J. Biomed. Sci.* 17:1.
- 819 Karere GM, Glenn JP, VandeBerg JL, Cox LA. 2012. Differential microRNA response to a high-  
820 cholesterol, high-fat diet in livers of low and high LDL-C baboons. *BMC Genomics* 13:1.
- 821 Kasaai B, Gaumond M-H, Moffatt P. 2013. Regulation of the Bone-restricted IFITM-like (Bril)  
822 Gene Transcription by Sp and Gli Family Members and CpG Methylation. *J. Biol. Chem.*  
823 288:13278–13294.
- 824 King MC, Wilson AC. 1975. Evolution at two levels in humans and chimpanzees. *Science*  
825 188:107–116.
- 826 Koch CM, Suschek CV, Lin Q, Bork S, Goergens M, Joussen S, Pallua N, Ho AD, Zenke M,  
827 Wagner W. 2011. Specific Age-Associated DNA Methylation Changes in Human Dermal  
828 Fibroblasts. *PLOS ONE* 6:e16679.
- 829 Kothapalli KSD, Anthony JC, Pan BS, Hsieh AT, Nathanielsz PW, Brenna JT. 2007. Differential  
830 Cerebral Cortex Transcriptomes of Baboon Neonates Consuming Moderate and High  
831 Docosahexaenoic Acid Formulas. Akbarian S, editor. *PLoS ONE* 2:e370.
- 832 Lea AJ, Altmann J, Alberts SC, Tung J. 2016. Resource base influences genome-wide DNA  
833 methylation levels in wild baboons (*Papio cynocephalus*). *Mol. Ecol.* 25:1681–1696.
- 834 Leek JT, Johnson WE, Parker HS, Jaffe AE, Storey JD. 2012. The sva package for removing  
835 batch effects and other unwanted variation in high-throughput experiments.  
836 *Bioinformatics* 28:882–883.
- 837 Leek JT, Storey JD. 2007. Capturing Heterogeneity in Gene Expression Studies by Surrogate  
838 Variable Analysis. *PLoS Genet.* 3:e161.
- 839 Leek JT, Storey JD. 2008. A general framework for multiple testing dependence. *Proc. Natl.*  
840 *Acad. Sci.* 105:18718–18723.
- 841 Leigh SR, Shea BT. 1995. Ontogeny and the evolution of adult body size dimorphism in apes.  
842 *Am. J. Primatol.* 36:37–60.
- 843 Lewton KL. 2017. The effects of captive versus wild rearing environments on long bone articular  
844 surfaces in common chimpanzees (*Pan troglodytes*). *PeerJ* 5:e3668.

- 845 Lewton KL, Ritzman T, Copes LE, Garland T, Capellini TD. 2018. Exercise-induced loading  
846 increases ilium cortical area in a selectively bred mouse model. *Am. J. Phys.*  
847 *Anthropol.*:1–9.
- 848 Lindskog C, Kuhlwilm M, Davierwala A, Fu N, Hegde G, Uhlén M, Navani S, Pääbo S, Pontén  
849 F. 2014. Analysis of candidate genes for lineage-specific expression changes in humans  
850 and primates. *J. Proteome Res.* 13:3596–3606.
- 851 Ling BMT, Bharathy N, Chung T-K, Kok WK, Li S, Tan YH, Rao VK, Gopinadhan S, Sartorelli  
852 V, Walsh MJ, et al. 2012. Lysine methyltransferase G9a methylates the transcription  
853 factor MyoD and regulates skeletal muscle differentiation. *Proc. Natl. Acad. Sci.*  
854 109:841–846.
- 855 Lister R, Pelizzola M, Dowen RH, Hawkins RD, Hon G, Tonti-Filippini J, Nery JR, Lee L, Ye Z,  
856 Ngo Q-M, et al. 2009. Human DNA methylomes at base resolution show widespread  
857 epigenomic differences. *Nature* 462:315–322.
- 858 Liu Y, Aryee MJ, Padyukov L, Fallin MD, Hesselberg E, Runarsson A, Reinius L, Acevedo N,  
859 Taub M, Ronninger M, et al. 2013. Epigenome-wide association data implicate DNA  
860 methylation as an intermediary of genetic risk in rheumatoid arthritis. *Nat. Biotechnol.*  
861 31:142–147.
- 862 Lönnstedt I, Speed T. 2002. Replicated microarray data. *Stat. Sin.* 12:31–46.
- 863 Loughlin J, Reynard LN. 2015. Osteoarthritis: Epigenetics of articular cartilage in knee and hip  
864 OA. *Nat. Rev. Rheumatol.* 11:6–7.
- 865 Macrini TE, Coan HB, Levine SM, Lerma T, Saks CD, Araujo DJ, Bredbenner TL, Coutts RD,  
866 Nicolella DP, Havill LM. 2013. Reproductive status and sex show strong effects on knee  
867 OA in a baboon model. *Osteoarthr. Cartil. OARS Osteoarthr. Res. Soc.* 21:839–848.
- 868 Madrid A, Chopra P, Alisch RS. 2018. Species-Specific 5 mC and 5 hmC Genomic Landscapes  
869 Indicate Epigenetic Contribution to Human Brain Evolution. *Front. Mol. Neurosci.*  
870 [Internet] 11. Available from:  
871 <https://www.frontiersin.org/articles/10.3389/fnmol.2018.00039/full>
- 872 Maksimovic J, Phipson B, Oshlack A. 2016. A cross-package Bioconductor workflow for  
873 analysing methylation array data. *F1000Research* 5:1281.
- 874 Martin DIK, Singer M, Dhahbi J, Mao G, Zhang L, Schroth GP, Pachter L, Boffelli D. 2011.  
875 Phyloepigenomic comparison of great apes reveals a correlation between somatic and  
876 germline methylation states. *Genome Res.* 21:2049–2057.
- 877 Mbalaviele G, Shin CS, Civitelli R. 2006. Perspective: Cell–Cell Adhesion and Signaling  
878 Through Cadherins: Connecting Bone Cells in Their Microenvironment. *J. Bone Miner.*  
879 *Res.* 21:1821–1827.
- 880 McCarthy DJ, Smyth GK. 2009. Testing significance relative to a fold-change threshold is a  
881 TREAT. *Bioinformatics* 25:765–771.
- 882 McCartney DL, Walker RM, Morris SW, McIntosh AM, Porteous DJ, Evans KL. 2016.  
883 Identification of polymorphic and off-target probe binding sites on the Illumina Infinium  
884 MethylationEPIC BeadChip. *Genomics Data* 9:22–24.
- 885 McHenry HM, Corruccini RS. 1978. The femur in early human evolution. *Am. J. Phys.*  
886 *Anthropol.* 49:473–487.
- 887 Mendizabal I, Shi L, Keller TE, Konopka G, Preuss TM, Hsieh T-F, Hu E, Zhang Z, Su B, Yi  
888 SV. 2016. Comparative Methylome Analyses Identify Epigenetic Regulatory Loci of  
889 Human Brain Evolution. *Mol. Biol. Evol.* 33:2947–2959.

- 890 Moazedi-Fuerst FC, Hofner M, Gruber G, Weinhaeusel A, Stradner MH, Angerer H, Peischler  
891 D, Lohberger B, Glehr M, Leithner A, et al. 2014. Epigenetic differences in human  
892 cartilage between mild and severe OA. *J. Orthop. Res.* 32:1636–1645.
- 893 Molaro A, Hodges E, Fang F, Song Q, McCombie WR, Hannon GJ, Smith AD. 2011. Sperm  
894 Methylation Profiles Reveal Features of Epigenetic Inheritance and Evolution in  
895 Primates. *Cell* 146:1029–1041.
- 896 Morris JA, Tsai P-C, Joehanes R, Zheng J, Trajanoska K, Soerensen M, Forgetta V, Castillo-  
897 Fernandez JE, Frost M, Spector TD, et al. 2017. Epigenome-wide association of DNA  
898 methylation in whole blood with bone mineral density. *J. Bone Miner. Res.*:n/a-n/a.
- 899 Oates NA, van Vliet J, Duffy DL, Kroes HY, Martin NG, Boomsma DI, Campbell M, Coulthard  
900 MG, Whitelaw E, Chong S. 2006. Increased DNA Methylation at the AXIN1 Gene in a  
901 Monozygotic Twin from a Pair Discordant for a Caudal Duplication Anomaly. *Am. J.*  
902 *Hum. Genet.* 79:155–162.
- 903 Ostanek B, Kranjc T, Lovšin N, Zupan J, Marc J. 2018. Chapter 18 - Epigenetic Mechanisms in  
904 Osteoporosis. In: Moskalev A, Vaiserman AM, editors. *Epigenetics of Aging and*  
905 *Longevity. Translational Epigenetics.* Boston: Academic Press. p. 365–388. Available  
906 from: <https://www.sciencedirect.com/science/article/pii/B9780128110607000188>
- 907 Pai AA, Bell JT, Marioni JC, Pritchard JK, Gilad Y. 2011. A Genome-Wide Study of DNA  
908 Methylation Patterns and Gene Expression Levels in Multiple Human and Chimpanzee  
909 Tissues. *PLOS Genet.* 7:e1001316.
- 910 Palacios D, Puri PL. 2006. The epigenetic network regulating muscle development and  
911 regeneration. *J. Cell. Physiol.* 207:1–11.
- 912 Pandorf CE, Haddad F, Wright C, Bodell PW, Baldwin KM. 2009. Differential epigenetic  
913 modifications of histones at the myosin heavy chain genes in fast and slow skeletal  
914 muscle fibers and in response to muscle unloading. *AJP Cell Physiol.* 297:C6–C16.
- 915 Paradis E, Claude J, Strimmer K. 2004. APE: Analyses of Phylogenetics and Evolution in R  
916 language. *Bioinforma. Oxf. Engl.* 20:289–290.
- 917 Perelman P, Johnson WE, Roos C, Seuánez HN, Horvath JE, Moreira MAM, Kessing B, Pontius  
918 J, Roelke M, Rumpler Y, et al. 2011. A Molecular Phylogeny of Living Primates. Brosius  
919 J, editor. *PLoS Genet.* 7:e1001342.
- 920 Petronis A, Gottesman II, Kan P, Kennedy JL, Basile VS, Paterson AD, Pependikyte V. 2003.  
921 Monozygotic twins exhibit numerous epigenetic differences: clues to twin discordance?  
922 *Schizophr. Bull.* 29:169–178.
- 923 Phipson B, Lee S, Majewski IJ, Alexander WS, Smyth GK. 2016. Robust hyperparameter  
924 estimation protects against hypervariable genes and improves power to detect differential  
925 expression. *Ann. Appl. Stat.* 10:946–963.
- 926 Prendergast JG, Campbell H, Gilbert N, Dunlop MG, Bickmore WA, Semple CA. 2007.  
927 Chromatin structure and evolution in the human genome. *BMC Evol. Biol.* 7:72.
- 928 Provencal N, Suderman MJ, Guillemin C, Massart R, Ruggiero A, Wang D, Bennett AJ, Pierre  
929 PJ, Friedman DP, Cote SM, et al. 2012. The Signature of Maternal Rearing in the  
930 Methylome in Rhesus Macaque Prefrontal Cortex and T Cells. *J. Neurosci.* 32:15626–  
931 15642.
- 932 Rakyan VK, Hildmann T, Novik KL, Lewin J, Tost J, Cox AV, Andrews TD, Howe KL, Otto T,  
933 Olek A, et al. 2004. DNA Methylation Profiling of the Human Major Histocompatibility  
934 Complex: A Pilot Study for the Human Epigenome Project. *PLOS Biol.* 2:e405.
- 935 Ralston SH, Uitterlinden AG. 2010. Genetics of Osteoporosis. *Endocr. Rev.* 31:629–662.

- 936 Ramos YFM, den Hollander W, Bovée JVMG, Bomer N, van der Breggen R, Lakenberg N,  
937 Keurentjes JC, Goeman JJ, Slagboom PE, Nelissen RGHH, et al. 2014. Genes Involved  
938 in the Osteoarthritis Process Identified through Genome Wide Expression Analysis in  
939 Articular Cartilage; the RAAK Study. *PLoS ONE* 9:1–12.
- 940 Rampersaud GC, Kauwell GP, Hutson AD, Cerda JJ, Bailey LB. 2000. Genomic DNA  
941 methylation decreases in response to moderate folate depletion in elderly women. *Am. J.*  
942 *Clin. Nutr.* 72:998–1003.
- 943 Reynard LN. 2017. Analysis of genetics and DNA methylation in osteoarthritis: What have we  
944 learnt about the disease? *Semin. Cell Dev. Biol.* 62:57–66.
- 945 Reynard LN, Bui C, Syddall CM, Loughlin J. 2014. CpG methylation regulates allelic expression  
946 of GDF5 by modulating binding of SP1 and SP3 repressor proteins to the osteoarthritis  
947 susceptibility SNP rs143383. *Hum. Genet.* 133:1059–1073.
- 948 Ritchie ME, Phipson B, Wu D, Hu Y, Law CW, Shi W, Smyth GK. 2015. limma powers  
949 differential expression analyses for RNA-sequencing and microarray studies. *Nucleic*  
950 *Acids Res.:*gkv007.
- 951 Ritzman TB, Banovich N, Buss KP, Guida J, Rubel MA, Pinney J, Khang B, Ravosa MJ, Stone  
952 AC. 2017. Facing the facts: The Runx2 gene is associated with variation in facial  
953 morphology in primates. *J. Hum. Evol.* 111:139–151.
- 954 Rivadeneira F, Styrkársdóttir U, Estrada K, Halldórsson BV, Hsu Y-H, Richards JB, Zillikens  
955 MC, Kavvoura FK, Amin N, Aulchenko YS, et al. 2009. Twenty bone-mineral-density  
956 loci identified by large-scale meta-analysis of genome-wide association studies. *Nat.*  
957 *Genet.* 41:1199–1206.
- 958 Rogers J, Gibbs RA. 2014. Comparative primate genomics: emerging patterns of genome content  
959 and dynamics. *Nat. Rev. Genet.* 15:347–359.
- 960 Romero IG, Ruvinsky I, Gilad Y. 2012. Comparative studies of gene expression and the  
961 evolution of gene regulation. *Nat. Rev. Genet.* 13:505–516.
- 962 Rushton MD, Reynard LN, Barter MJ, Refaie R, Rankin KS, Young DA, Loughlin J. 2014.  
963 Characterization of the Cartilage DNA Methylome in Knee and Hip Osteoarthritis:  
964 Methylation Profile of OA Cartilage. *Arthritis Rheumatol.* 66:2450–2460.
- 965 Schultz AH. 1930. The Skeleton of the Trunk and Limbs of Higher Primates. *Hum. Biol.* 2:303–  
966 438.
- 967 Schultz AH. 1937. Proportions, Variability and Asymmetries of the Long Bones of the Limbs  
968 and the Clavicles in Man and Apes. *Hum. Biol.* 9:281–328.
- 969 Sharif J, Endo TA, Toyoda T, Koseki H. 2010. Divergence of CpG island promoters: A  
970 consequence or cause of evolution? *Dev. Growth Differ.* 52:545–554.
- 971 Shelnutt KP, Kauwell GPA, Gregory III JF, Maneval DR, Quinlivan EP, Theriaque DW,  
972 Henderson GN, Bailey LB. 2004. Methylenetetrahydrofolate reductase 677C→T  
973 polymorphism affects DNA methylation in response to controlled folate intake in young  
974 women. *J. Nutr. Biochem.* 15:554–560.
- 975 Simon TC, Jeffries MA. 2017. The Epigenomic Landscape in Osteoarthritis. *Curr. Rheumatol.*  
976 *Rep.* 19:30.
- 977 Singer M, Kosti I, Pachter L, Mandel-Gutfreund Y. 2015. A diverse epigenetic landscape at  
978 human exons with implication for expression. *Nucleic Acids Res.:*gkv153.
- 979 Slieker RC, Bos SD, Goeman JJ, Bovée JV, Talens RP, van der Breggen R, Suchiman HED,  
980 Lameijer E-W, Putter H, van den Akker EB, et al. 2013. Identification and systematic

- 981 annotation of tissue-specific differentially methylated regions using the Illumina 450k  
982 array. *Epigenetics Chromatin* 6:26.
- 983 Smith RWA, Monroe C, Bolnick DA. 2015. Detection of Cytosine Methylation in Ancient DNA  
984 from Five Native American Populations Using Bisulfite Sequencing. *PLoS ONE*  
985 [Internet] 10. Available from: <http://www.ncbi.nlm.nih.gov/pmc/articles/PMC4445908/>
- 986 Smith SM, Garic A, Berres ME, Flentke GR. 2014. Genomic factors that shape craniofacial  
987 outcome and neural crest vulnerability in FASD. *Front. Genet.* [Internet] 5. Available  
988 from: <http://journal.frontiersin.org/article/10.3389/fgene.2014.00224/abstract>
- 989 Smyth GK. 2004. Linear models and empirical bayes methods for assessing differential  
990 expression in microarray experiments. *Stat. Appl. Genet. Mol. Biol.* 3:Article3.
- 991 Suter CM, Martin DIK, Ward RL. 2004. Germline epimutation of MLH1 in individuals with  
992 multiple cancers. *Nat. Genet.* 36:497–501.
- 993 Suzuki MM, Bird A. 2008. DNA methylation landscapes: provocative insights from  
994 epigenomics. *Nat. Rev. Genet.* 9:465–476.
- 995 Terzidis I, Totlis T, Papathanasiou E, Sideridis A, Vlasis K, Natsis K. 2012. Gender and Side-to-  
996 Side Differences of Femoral Condyles Morphology: Osteometric Data from 360  
997 Caucasian Dried Femori. *Anat. Res. Int.* 2012:e679658.
- 998 Tung J, Zhou X, Alberts SC, Stephens M, Gilad Y. 2015. The genetic architecture of gene  
999 expression levels in wild baboons. *eLife* 4:e04729.
- 1000 Uebbing S, Künstner A, Mäkinen H, Backström N, Bolivar P, Burri R, Dutoit L, Mugal CF,  
1001 Nater A, Aken B, et al. 2016. Divergence in gene expression within and between two  
1002 closely related flycatcher species. *Mol. Ecol.* 25:2015–2028.
- 1003 Vilgalys TP, Rogers J, Jolly C, Mukherjee S, Tung J. 2018. Evolution of DNA methylation in  
1004 baboons. Available from: <http://biorxiv.org/lookup/doi/10.1101/400093>
- 1005 Warner LR, Babbitt CC, Primus AE, Severson TF, Haygood R, Wray GA. 2009. Functional  
1006 consequences of genetic variation in primates on tyrosine hydroxylase (TH) expression in  
1007 vitro. *Brain Res.* 1288:1–8.
- 1008 Weber M, Hellmann I, Stadler MB, Ramos L, Pääbo S, Rebhan M, Schübeler D. 2007.  
1009 Distribution, silencing potential and evolutionary impact of promoter DNA methylation  
1010 in the human genome. *Nat. Genet.* 39:457–466.
- 1011 Weksberg R, Shuman C, Caluseriu O, Smith AC, Fei Y-L, Nishikawa J, Stockley TL, Best L,  
1012 Chitayat D, Olney A, et al. 2002. Discordant KCNQ1OT1 imprinting in sets of  
1013 monozygotic twins discordant for Beckwith-Wiedemann syndrome. *Hum. Mol. Genet.*  
1014 11:1317–1325.
- 1015 White T, Folkens P. 2000. *Human osteology*. 2nd ed. San Diego: Academic Press
- 1016 Whitehead A, Crawford DL. 2006. Neutral and adaptive variation in gene expression. *Proc. Natl.*  
1017 *Acad. Sci. U. S. A.* 103:5425–5430.
- 1018 Young MD, Wakefield MJ, Smyth GK, Oshlack A. 2010. Gene ontology analysis for RNA-seq:  
1019 accounting for selection bias. *Genome Biol.* 11:R14.
- 1020 Zeng J, Konopka G, Hunt BG, Preuss TM, Geschwind D, Yi SV. 2012. Divergent Whole-  
1021 Genome Methylation Maps of Human and Chimpanzee Brains Reveal Epigenetic Basis  
1022 of Human Regulatory Evolution. *Am. J. Hum. Genet.* 91:455–465.
- 1023 Zhang Bo, Zhou Y, Lin N, Lowdon RF, Hong C, Nagarajan RP, Cheng JB, Li D, Stevens M, Lee  
1024 HJ, et al. 2013. Functional DNA methylation differences between tissues, cell types, and  
1025 across individuals discovered using the M&M algorithm. *Genome Res.* 23:1522–1540.

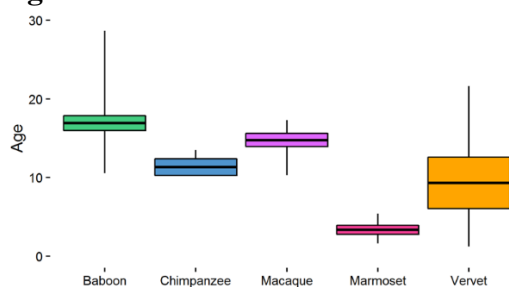
1026 Zwetsloot KA, Laye MJ, Booth FW. 2009. Novel epigenetic regulation of skeletal muscle  
1027 myosin heavy chain genes. Focus on “Differential epigenetic modifications of histones at  
1028 the myosin heavy chain genes in fast and slow skeletal muscle fibers and in response to  
1029 muscle unloading.” *AJP Cell Physiol.* 297:C1–C3.

1030

1031 **Figures:**

1032

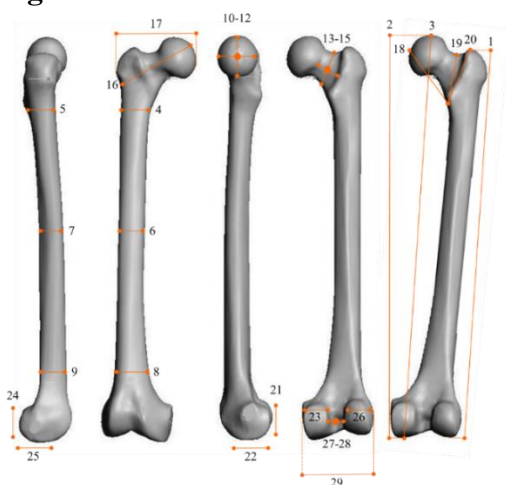
1033 **Figure 1.**



1034

1035

1036 **Figure 2.**

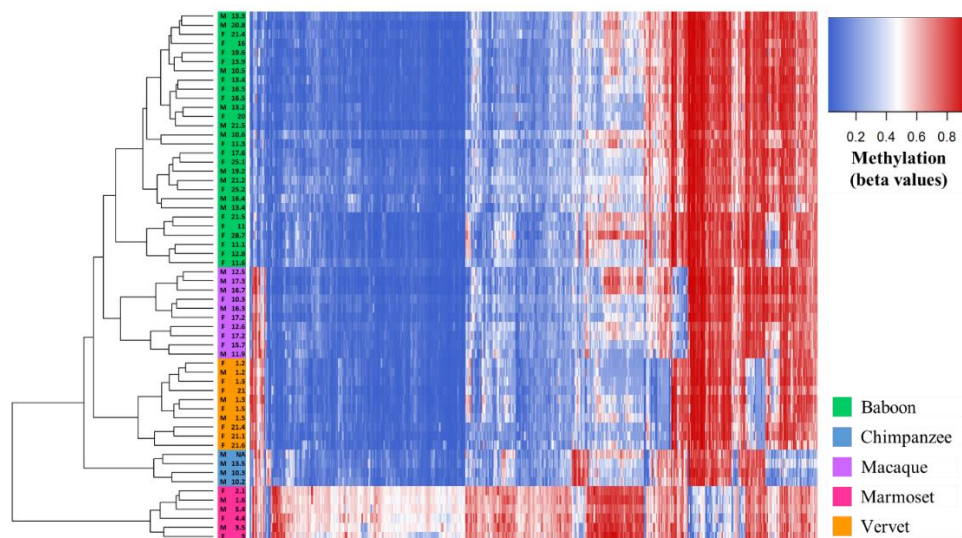


1037

1038

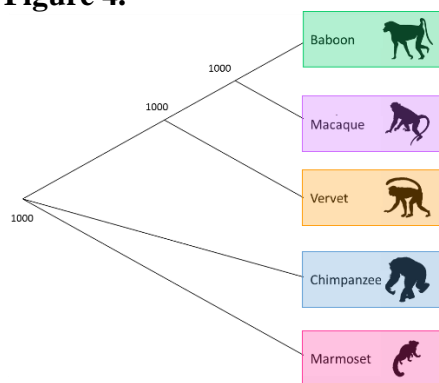
1039 **Figure 3.**





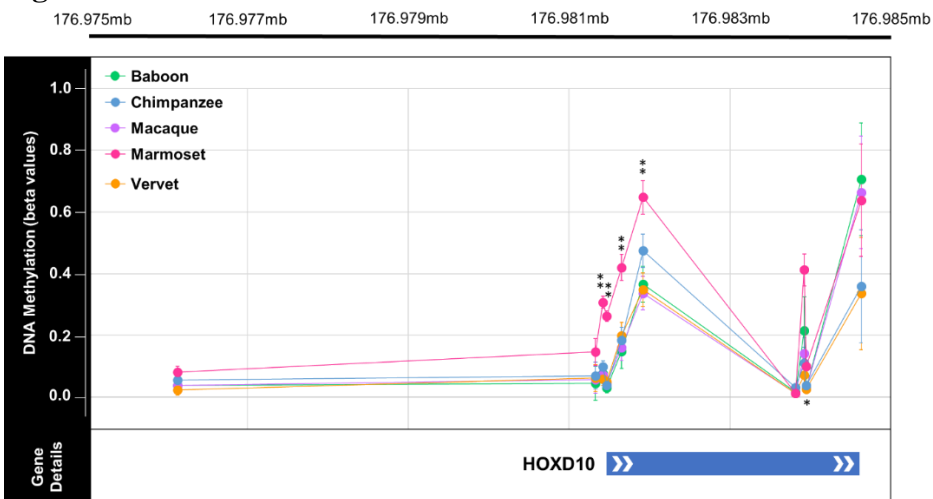
1040  
1041  
1042

**Figure 4.**



1043  
1044  
1045

**Figure 5.**



1046  
1047  
1048

**Figure 6.**



1049  
1050

### Figure Legends:

1051

1052

1053

1054

1055

1056

1057

1058

1059

1060

1061

1062

1063

1064

1065

1066

1067

1068

1069

1070

1071

1072

1073

1074

1075

1076

1077

1078

**Figure 1. Nonhuman Primate Sample Set Ages.** Boxes represent one standard deviation from the average age, and whiskers depict the full range of ages for each species. Baboons (n=28) are  $16.90 \pm 5.02$  years, chimpanzees (n=4) are  $11.31 \pm 1.87$  years, macaques (n=10) are  $14.75 \pm 2.65$  years, marmosets (n=6) are  $3.34 \pm 1.41$  years, and vervets (n=10) are  $9.31 \pm 10.30$  years. Additional details can be found in Table S1.

**Figure 2. Nonhuman Primate Morphological Measurements.** See Table S6 for a detailed description of these measurements.

**Figure 3. Methylation Levels at Species-Specific DMPs with  $\Delta\beta \geq 0.4$  Identified in the Inter-Specific Study.** Heatmap depicting the DNA methylation levels ( $\beta$  values) of all species-specific DMPs with average absolute  $\Delta\beta$  values greater than 0.4 between each taxonomic group (x-axis) in all nonhuman primate samples (n=58). The sex and age of each nonhuman primate are also provided (y-axis). Red indicates higher methylation at a DMP, while blue indicates lower methylation at a DMP. The dendrogram of all samples (y-axis) clusters individuals based on the similarity of their methylation patterns. Samples cluster based on species-level taxonomic groupings and as predicted based on known species phylogenetic histories.

**Figure 4. Phylogeny Based on Average Species-Level Global Changes in Methylation.** Observed phylogenetic relationship among nonhuman primates when considering average species-level global changes in methylation. This tree was constructed using the methylation levels for all finalized 39,802 filtered probes. I averaged the  $\beta$  values per probe within a species, used Euclidean distances to calculate the difference between every two species, and estimated a neighbor joining tree using this distance matrix. For the resulting tree, 1000 bootstraps were performed to determine confidence values for each branch. The number provide at each node indicates the number of bootstrap replicates that support it out of the 1000 performed.

1079

1080 **Figure 5. Genome-Wide Methylation Levels Across *HOXD10* in Nonhuman Primates.** Plot  
1081 of the methylation levels of significant DMPs across the *HOXD10* gene (hg19 chr2:176981492-  
1082 176984670). Plot shows the average  $\beta$  values for each DMP with error bars indicating 1 standard  
1083 deviation in each direction for each comparative group (teal = baboon, orange = chimpanzee,  
1084 purple = macaque, pink = marmoset, and light green = vervet). DMP chromosomal position in  
1085 relation to the *HOXD10* gene is also depicted. This gene is of interest because it has been found  
1086 to be differential methylation in ancient and modern hominin species (Gokhman et al. 2014). Of  
1087 the sites depicted here, 5 DMPs were found to show significant species-specific methylation in  
1088 marmosets. Of the 5 species-specific DMPs in the *HOXD10* gene of marmosets, 4 have  $\Delta\beta$   
1089 between 0.2 and 0.3 (\*\*) and 1 has a  $\Delta\beta < 0.1$  (\*). See Table S13 for additional information.

1090

1091 **Figure 6. Gene-Specific Methylation Levels Across *HOXD10* in Nonhuman Primates.** Bar  
1092 plot of DNA methylation across the *HOXD10* gene (hg19 chr2:176981492-176984670), as well  
1093 as upstream and downstream several hundred bases (hg19 chr2:176980532-176985117). Bars  
1094 depict the presence (tall bar), partial presence (medium bar), or absence (low bar) of methylation  
1095 at human derived CpG sites in 15 nonhuman primate samples – 3 baboons, 3 macaques, 3  
1096 vervets, 3 chimpanzees, and 3 marmosets. While regular sequencing was very successful,  
1097 bisulfite sequencing was less successful, with several sequence reads uninterpretable. As such,  
1098 nonhuman primate methylation data is only available for a subset of the CpGs known in humans.  
1099 Partial presence of methylation was called when sequencing fluorescence peaks for cytosine and  
1100 thymine were both present at a particular site and one was at least half the size of the other.  
1101 Overall, these data provide additional information regarding gene-specific methylation levels  
1102 across *HOXD10*. CpG sites that were also targeted by the EPIC array are highlighted in yellow  
1103 and include cg18115040 (chr2, position 176981328), cg25371634 (chr2, position 176981422),  
1104 cg13217260 (chr2, position 176981469), cg03918304 (chr2, position 176981654), cg17489939  
1105 (chr2, position 176981919), cg26708100 (chr2, position 176983815), cg10393811 (chr2,  
1106 position 176983927), cg08992581 (chr2, position 176983949), and cg06005169 (chr2, position  
1107 176984634). See Table S18 and Files S8-S9 for additional information.